

Theory of the electromagnetic production of hyperons ¹

Petr Bydžovský and Dalibor Skoupil

Nuclear Physics Institute of the ASCR, Řež, 250 68, Czech Republic

Abstract

Some basic properties of isobar models are discussed using the Saclay-Lyon, Kaon-MAID, and H2 models and a comparison of their predictions with experimental data is given for photo- and electroproduction of K^+ on the proton and for photoproduction of K^0 on the deuteron in specific kinematical regions. Results of the isobar models are also compared with the Regge-isobar hybrid model, Regge-plus-resonance.

Keywords: photo and electroproduction of hyperons, baryon resonances, isobar model, Regge-plus-resonance model

1. Introduction

Production of the Λ and Σ hyperons on nucleons and nuclei induced by the electron beam provides completing information about properties of baryons and their behavior in nuclei. Besides the study of the reaction mechanism, a correct description of the elementary production on nucleons is important for minimizing uncertainties in calculations of the excitation spectra for electroproduction of hypernuclei [1, 2].

There are various methods of description of the elementary production process. Among them the single-channel description based on an effective Lagrangian considering only hadronic degrees of freedom is of special importance because the corresponding isobar model can be easily utilized in the calculations of hypernucleus electroproduction [1]. Analyses of data with the isobar model provide information about properties of nucleon resonances and

¹Presented at the 11th International Conference on Hypernuclear and Strange Particle Physics, 1 - 5 October, 2012, Barcelona.

the existence of “missing resonances” predicted by the quark model but not observed in other processes [3, 4].

In the hadrodynamical approach, several production channels are coupled by the final-state meson-baryon interaction and should be treated simultaneously. In this coupled-channel approach [5], rescattering effects in the meson-baryon system in intermediate states can be included. Considerable simplification originates in neglecting the rescattering effects in the formalism assuming that these effects are included to some extent by means of effective values of the coupling constants fitted to experimental data. This simplifying assumption was adopted in many isobar models, e.g., Saclay-Lyon (SL) [6], Kaon-MAID (KM) [3, 7], and Gent [8].

Another approach to description of the process, suited also for energies above the nucleon-resonance region up to $E_\gamma^{lab} \approx 16$ GeV, is the hybrid Regge-plus-resonance model [9, 10, 11] (RPR). This model combines the Regge model [12], appropriate to description above the resonance region ($E_\gamma^{lab} > 4$ GeV), with elements of the isobar model eligible for the lower-energy region.

In the quark models for photoproduction of kaons [13], resonances are implicitly included as excited states and therefore a number of free parameters is relatively small. Another asset of this approach is a natural description of a hadron internal structure which have to be modeled phenomenologically via form factors in the isobar models. However, the quark models for the electromagnetic production of kaons are too complicated for their further use in the calculations of hypernucleus electroproduction.

2. Isobar and Regge-plus-resonance models

In the isobar model the amplitude is constructed as a sum of the tree-level Feynman diagrams which can be divided into the nonresonant and resonant contributions. The former consists of the Born terms and exchanges of kaon (t-channel) and hyperon (u-channel) resonances. The latter is modeled by exchanges of nucleon resonances in s-channel. The problem of the isobar model for kaon photoproduction is a too large contribution from the Born terms which has to be reduced assuming some mechanism [8]. One possibility is to include several hyperon resonances which counterbalance the Born contribution [6, 14]. Another way is to assume hadronic form factors (hffs) in the strong (baryon-meson-baryon) vertices [3, 7] which suppress the Born terms very strongly. In the Gent isobar model a combination of both mechanisms

is used [8]. Besides a reduction of the Born terms the hffs can model an internal structure of hadrons in the strong vertices neglected in the effective Lagrangian. The form factors are included by a gauge-invariant technique [15] assuming the dipole [7, 8], Gaussian [9] or multidipole-Gauss [10, 11] types. These various methods of reduction of the Born terms influence strongly a dynamics of the isobar model. The problem of the large Born contributions is avoided in the RPR approach.

Here we will discuss results of the KM, Saclay-Lyon A (SLA) [14], and H2 [4] models. These models include the Born diagrams and contributions from exchanges of the $K^*(890)$ and $K_1(1270)$ resonances. The main coupling constants, $g_{KN\Lambda}$ and $g_{KN\Sigma}$, fulfill the limits of 20% broken SU(3) symmetry [6]. These models differ in a selection of the s - and u -channel resonances, in a treatment of the hadron structure, and in a set of experimental data to which the free parameters were adjusted. In the SLA model only one nucleon, $P_{13}(1720)$, and four hyperon, $S_{01}(1407)$, $S_{01}(1670)$, $P_{01}(1810)$, and $P_{11}(1660)$, resonances are included whereas in KM four nucleon, $S_{11}(1650)$, $P_{11}(1710)$, $P_{13}(1720)$, and $D_{13}(1895)$, and no hyperon resonances are assumed [7]. The H2 model includes the same nucleon resonances as KM plus two hyperon resonances, $S_{01}(1670)$ and $S_{01}(1800)$ [4]. In SLA hadrons are treated as point-like objects but in the KM and H2 models the dipole-type hffs are included in the baryon-meson-baryon vertices. The models provide reasonable results for photon laboratory energies below 2.2 GeV, see, e.g., analysis of data with the SL and KM models in Ref. [2].

In the RPR model for $K^+\Lambda$ production, the nonresonant part of the amplitude is modeled by exchanges of two strongly degenerate $K^+(494)$ and $K^{*+}(892)$ trajectories as in the Regge model [12] where the corresponding propagators can be assumed either with a constant (1) or rotating ($e^{-i\pi\alpha(t)}$, $\alpha(t)$ is the Regge trajectory) phase [9, 11]. This phase ambiguity could not be removed in the version RPR-2007 [9] using the standard least-squares approach in an analysis of high-energy data but, applying the Bayesian inference method in the analysis [16, 11], the rotating phases were unambiguously assigned to both propagators in the new versions RPR-2011A and RPR-2011B [11]. In addition, to maintain gauge invariance in the RPR model, the amplitude includes the electric part of the proton exchange which is reggeised in the same way as the kaon exchange [9, 11, 12]. The three free parameters of background, the pseudo-scalar coupling constant of the K^+ trajectory and the vector and tensor coupling constants of the K^* trajectory, are determined by fitting to photoproduction data above the resonance

region ($\sqrt{s} = W > 2.6$ GeV) [9, 10, 11].

The resonant part of the amplitude is described by exchanges of nucleon resonances like in the isobar model. A smooth transition from the resonant region into the high-energy Regge region is assured by strong hffs of Gaussian [9] or multidipole-Gauss [10, 11] type. In the robust analysis of the world's photoproduction data based on the Bayesian evidence two sets of nucleon resonances with highest probabilities of contributing to the reaction mechanism were selected from the 2048 considered model variants [10]. These sets of nucleon resonances constitute the new versions of the Gent RPR model, RPR-2011A with eight resonances and RPR-2011B with five resonances [11].

Important merit of the RPR model, besides that it describes satisfactorily the experimental data in the broad energy region from threshold up to $E_\gamma^{lab} \approx 16$ GeV ($W = 5.56$ GeV), is absence of the large Born contribution in the nonresonant part of the amplitude. Therefore, no hffs for the background are needed making a difference in the reaction mechanism of the RPR model and the isobar model with hffs. This difference appears to be important for description of the cross sections at very small kaon angles as we will discuss in the next section.

3. Discussion of results

The different mechanism of reducing the large contribution of the Born terms in the SLA and KM models plays an important role in description of the $n(\gamma, K^0)\Lambda$ reaction as it is demonstrated in Fig. 1. In the $K^0\Lambda$ photoproduction the Born contribution reveals a different angular dependence than in the $K^+\Lambda$ channel due to absence of the kaon exchange and to a significant modification of the nucleon exchange (the electric part is missing and the anomalous magnetic moment changes its sign: $\mu_p = 1.79 \rightarrow \mu_n = -1.92$). In SLA the hyperon exchanges cannot counterbalance the large backward peaked Born contribution as they do in the $K^+\Lambda$ channel but now this effect can be provided by the K_1 exchange, see Fig. 1a. The SLA model is very sensitive to the strength of the K_1 contribution as shown in Ref. [18] which can be tuned to the deuteron data [17]. In the KM model, the Born contribution is strongly reduced by hffs as in the $K^+\Lambda$ channel and the K_1 exchange does not play a significant role, Fig. 1b. This makes a notably smaller sensitivity to the strength of K_1 contribution in the KM model than in SLA [18]. The H2 model appears to be still less sensitive, see Fig.5 in Ref. [18].

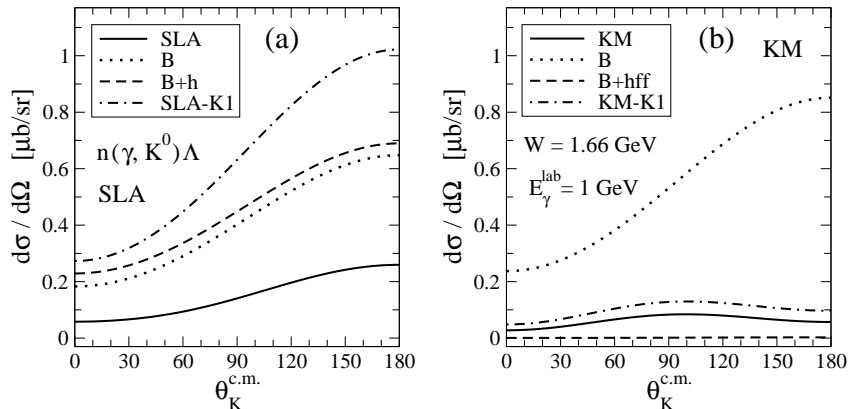


Figure 1: Dynamics of the SLA (a) and KM (b) models in $n(\gamma, K^0)\Lambda$ at $E_\gamma^{lab} = 1$ GeV. Contributions from the Born terms (B) are slightly modified by hyperon exchanges in SLA (B+h) but strongly reduced by hadronic form factors in KM (B+hff). Solid and dash-dotted lines show results of entire models and results without the K_1 exchange, respectively. The parameter of the K_1^0 exchange in SLA is from Ref. [17] ($r_{K_1 K\gamma} = -1.405$) and in KM the original value from Ref. [7] is used ($r_{K_1 K\gamma} = -0.45$).

In Fig. 2, we show results of the SLA, KM2 (our version of the Kaon-MAID model, see below), and H2 models for K^0 photoproduction on the neutron (a) and deuteron (b). In these models the ratio of the electromagnetic coupling constants for the neutral and charged modes of K_1 , $r_{K_1 K\gamma}$ [17], was fitted to the deuteron data in the low energy bin (Fig. 2b) where the production of Σ hyperons is negligible [17]. The energy-averaged and angle-integrated momentum distribution of the $K^0\Lambda$ production on deuteron was calculated in PWIA [18]. The corresponding fitted values of $r_{K_1 K\gamma}$ are -1.41, 0.47, and 7.75, for the SLA, KM2, and H2 models, respectively. A model dependence of this ratio, which can be related with a ratio of the decay widths of K_1 [17, 18], is apparent. The large value for H2 is evoked by a very small sensitivity of H2 to this parameter in this energy region [18]. Note also the opposite sign of the ratio for the Kaon-MAID model with respect to the original value of -0.45 [7] used in Fig. 1.

The models give different predictions for the elementary cross section in the backward hemisphere, see Fig. 2a, which results in different shapes of the momentum distributions for kaon laboratory momenta $0.1 < p_K < 0.4$ GeV/c, Fig. 2b. The excess of the elementary cross sections in the forward hemisphere for the KM2 and H2 models is seen for $0.4 < p_K < 0.6$ GeV/c.

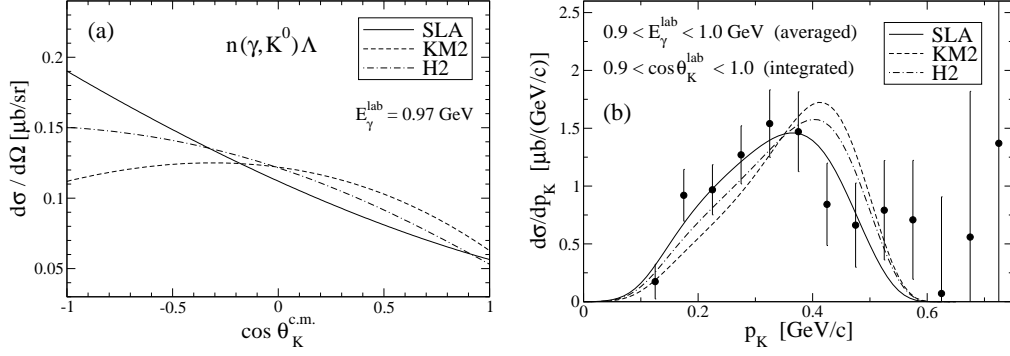


Figure 2: Angular dependence of the c.m. cross sections for $n(\gamma, K^0)\Lambda$ is shown in (a) for the SLA, KM2, and H2 models (see text for more details). PWIA calculations [18] of the energy-averaged and kaon-angle integrated momentum distributions for $d(\gamma, K^0)\Lambda p$ are compared with data on $d(\gamma, K^0)YN$ [17] in (b). Contributions from the $\Sigma^0 p$ and $\Sigma^+ n$ channels are negligible in this energy region [17].

Both Kaon-MAID and H2 models are not able to describe satisfactorily the deuteron data, even after fitting the $r_{K_1 K \gamma}$ parameter, which can be attributed to the applied method of reduction of the Born terms. The SLA model fits the shape of distribution very well with $\chi^2/n.d.f. = 0.64$ in contrary to 1.09 and 1.75 for H2 and KM2, respectively.

Predictions of the SLA, KM2, and H2 models for inclusive photoproduc-

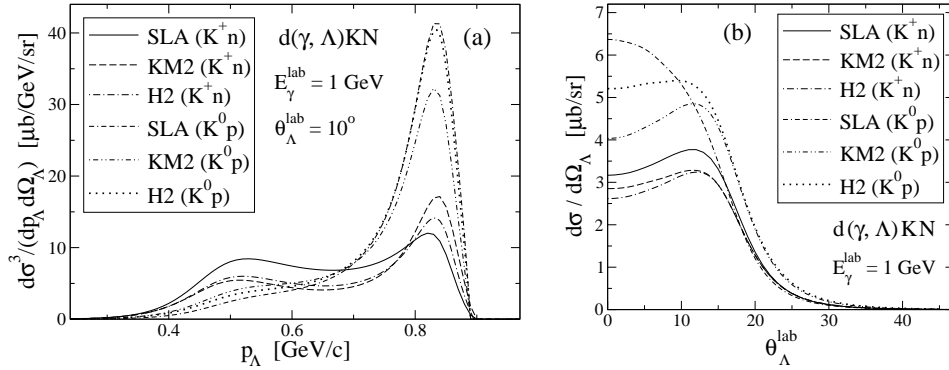


Figure 3: Λ -momentum distribution at Λ angle 10° (a) and Λ -momentum-integrated angular distribution (b) with K^+n and K^0p final states in $d(\gamma, \Lambda)KN$ as predicted by the SLA, KM2 and H2 models (see text for more details).

tion of Λ on deuteron are given in Fig. 3 for photon laboratory energy 1 GeV, displaying separately results with the K^+n and K^0p final states. For the Λ angle of 10° , the models predict similar shapes of the momentum distribution both in the K^+ and K^0 production, Fig. 3a. Results of the Λ -momentum integrated cross sections in Fig. 3b are also very similar for the K^+ production on proton in the whole angular range but the angular dependences differ for the K^0 production on neutron (K^0p final state) at Λ angles smaller than 15° . All three models predict larger cross sections for photoproduction on the neutron than on the proton.

In Fig. 4 results of the isobar and RPR models for photoproduction of K^+ on the proton are compared with data for the photon laboratory energies in the resonance region, 1.3 and 2.2 GeV, and in the Regge region at 8 GeV. Note the problem of normalization of SLAC data [25] which, we suppose, do not affect too much their angular dependence. For the RPR models we adopted the version RPR-2+D₁₃ [9] (RPR-2007) fitted to the forward-angle data and our fits RPR-1 and RPR-2. These new RPR models include the nucleon resonances $S_{11}(1535)$, $S_{11}(1650)$, $P_{11}(1710)$, $P_{13}(1720)$, and $D_{13}(1895)$ which were selected in the version RPR-2011B of the Gent RPR

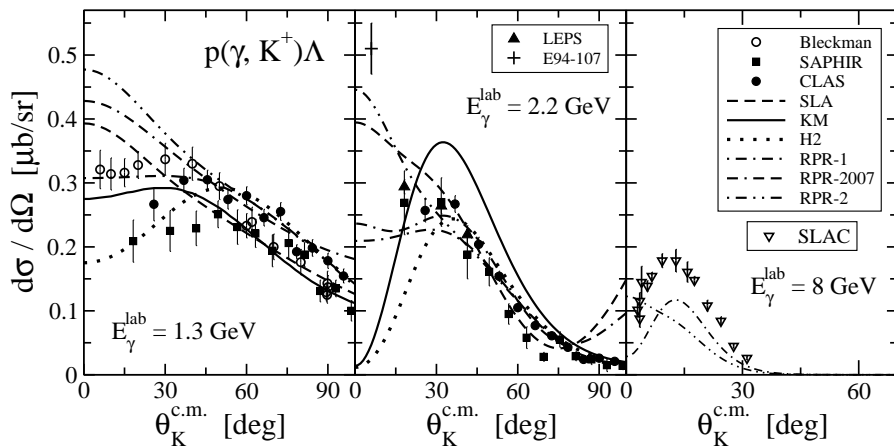


Figure 4: Results of isobar and Regge-plus-resonance models for the cross sections in $p(\gamma, K^+)\Lambda$ are compared with data in the resonance region, Bleckman [19], SAPHIR [20], CLAS [21], and LEPS [22], and above this region, SLAC [23]. The Jlab Hall A data point (E94-107) [24] is for electroproduction very near to the photoproduction point, $Q^2 = 0.07$ (GeV/c)², at $E_\gamma^{\text{lab}} = 2.15$ GeV.

model [11] and which, except for the first subthreshold resonance $S_{11}(1535)$, are also used in the isobar models KM and H2. In the new RPR models the multidipole-Gauss hffs were used as in RPR-2011B. Both models were fitted to the cross sections from the CLAS and LEPS data sets; RPR-1 to data of the whole angular range and RPR-2 only to the forward-angle data ($\theta_K < 90^\circ$). The models differ mainly in description of the nonresonant part of the amplitude. Both magnitudes and signs of the coupling constants of K and K^* trajectories differ in these models which appears to be important for predictions of the cross sections at very small kaon angles and higher energies, see Fig. 4.

In the resonance region, results of the models markedly differ for kaon angles smaller than 40° , which is more apparent at the larger energy 2.2 GeV (Fig. 4). At this energy, the isobar models with hffs, KM and H2, reveal a strong reduction of the cross section due to suppression of the proton exchange by the hffs. On the contrary, the SLA model predicts a forward peaked cross section similarly as the Regge-like model RPR-2. A differentiation of predictions of isobar models with and without hffs for $E_\gamma^{lab} > 1.5$ GeV is apparent from the energy dependence of the cross sections for a very forward-angle in Fig. 5 (see also Fig. 2 in Ref. [18] for more isobar models).

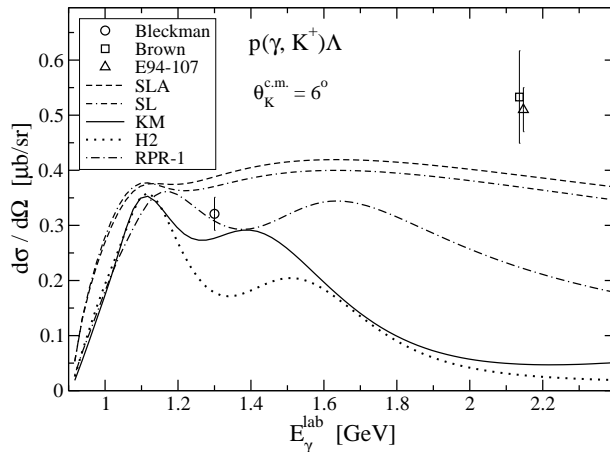


Figure 5: Photon-energy dependent c.m. photoproduction cross sections at c.m. kaon angle 6° as predicted by isobar models and RPR-1. The data point 'Bleckman' is for photoproduction [19] and the points 'Brown' [26] and 'E94-107' [24] for electroproduction with very small Q^2 .

The lack of experimental data in this kinematical region, $\theta_K^{c.m.} \approx 6^\circ$, does not allow to test reliably the models [2] and therefore to minimize uncertainties in the calculations of the cross sections for electroproduction of hypernuclei [1].

The steep angular dependence for near zero angles predicted by SLA and RPR-2 in Fig. 4 is supported by the electroproduction data point E94-107 at $E_\gamma^{lab} = 2.15$ GeV ($W = 2.2$ GeV) induced by almost a real photon with $Q^2 = 0.07$ (GeV/c)² [24]. A conservative estimation of contributions from the longitudinal amplitudes gives for the particular kinematics the value of the transversal cross section (corresponding to the photoproduction cross section), $\sigma_T \approx 0.38$ $\mu\text{b/sr}$ [24], which still favours the models SLA and RPR-2. The forward peaking of the cross section is also consistent with conclusions from the analysis of CLAS data [21]. The authors concluded that in the energy region $2.3 < W < 2.6$ GeV (2.6 GeV is the maximum energy in the experiment) the cross section is dominantly forward peaked which can be interpreted as a substantial contribution to the reaction mechanism by t -channel exchange. The other two Regge-like models, RPR-1 and RPR-2007, predict a plateau at small angles in the 2.2 GeV region showing that the Regge-based modeling of the nonresonant part of amplitude can also provide other type of the angular dependence. Note that the SLA model is very successful in predicting reasonable values of the cross sections for the electroproduction of hypernuclei [27] which points out to its realistic description of the elementary process at very forward kaon angles (dominating the hypernucleus production) and c.m. energies around 2.2 GeV.

However, in the higher energy region, $E_\gamma^{lab} = 8$ GeV in Fig. 4 ($W = 3.99$ GeV), the SLAC data [23] reveal rather the inverse angular dependence than that observed in the resonance region at $E_\gamma^{lab} = 2.2$ GeV ($W = 2.24$ GeV) and in Ref. [21]. Therefore, the SLAC data, if their angular dependence will not change too much in a re-analysis due to the normalization, suggest that the RPR-1 model gives a correct angular dependence at very small kaon angles rather than RPR-2 which would mean that at 2.2 GeV a flat angular dependence (a plateau) is a more realistic behaviour of the cross section. It is obvious that new good quality experimental data for kaon c.m. angles $0 - 20^\circ$ and in some energy region, e.g., $2 < W < 3$ GeV, are needed to better understand the reaction mechanism at the very-forward-angle region.

In electroproduction, aside from appropriate electromagnetic form factors, additional possible couplings of the virtual photon with baryons, e.g., the “longitudinal couplings” (LC), should be included in the effective Lagrangian and the corresponding coupling constants should be fitted to the

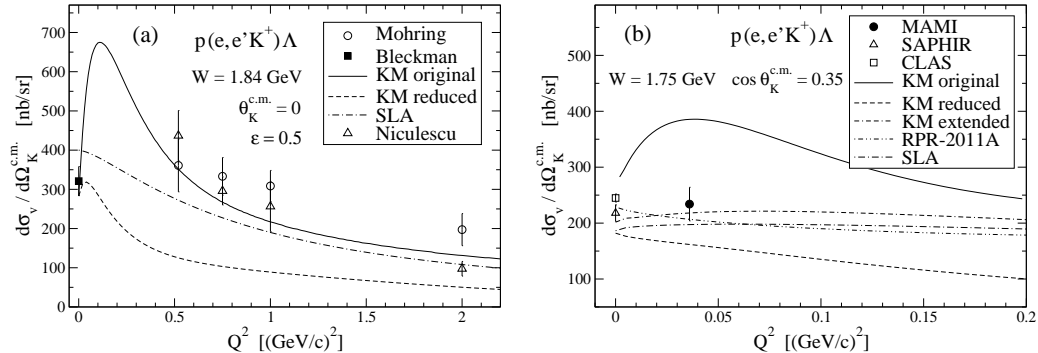


Figure 6: Predictions of the isobar and Regge-plus-resonance models for the full unpolarized electroproduction cross section are compared with photoproduction data Bleckman (for $\theta_K^{c.m.} = 6^\circ$) [19], SAPHIR [20], and CLAS [21] and with electroproduction data Mohring [30], Niculescu [29], and MAMI [28], to show a Q^2 dependence of the cross section for $0 < Q^2 < 2.2$ (GeV/c) 2 (a) and near the photoproduction point ($Q^2=0$) (b).

Q^2 dependence of electroproduction cross section. This was done for the Kaon-MAID model using data by Niculescu et al [29]. The KM result, “KM original”, for the full cross section at the zero kaon angle, $\sigma_T + \epsilon \sigma_L$ with $\epsilon = 0.5$, and at $W = 1.84$ GeV is shown in Fig. 6a in comparison with the SLA model, the data by Niculescu et al, the re-analyzed data by Mohring et al [30], and the photoproduction data point by Bleckmann et al for $\theta_K^{c.m.} = 6^\circ$ [19]. The data by Mohring et al do not reveal such a steep Q^2 dependence as the data by Niculescu et al suggesting a smoother transition between the photoproduction point ($Q^2 = 0$) and the electroproduction data. The sharp bump for $0 < Q^2 < 0.5$ (GeV/c) 2 seen in the result of KM is modeled by strong LC as it is apparent from comparison with the version “KM reduced” in which these couplings were removed. The SLA model, which does not include LC, predicts a smooth Q^2 dependence at zero kaon angle, however, overestimating the photoproduction data point for $\theta_K^{c.m.} = 6^\circ$ at this energy. Behavior of the full cross section near the photoproduction point for kaon c.m. angle about 70° is shown in Fig. 6b. The MAMI data [28] collected for a very small value of Q^2 at $W = 1.75$ GeV but nonzero kaon angles, $0.15 < \cos \theta_K < 0.65$, suggest a smooth Q^2 dependence which means that contributions from LC are not too big in the investigated kinematical region. Therefore, the models without LC can give reasonable results also for the electroproduction cross sections [28]. The new version of Kaon-MAID model, “KM extended”, with

reduced strength of LC is very well consistent with the new data and results from the models RPR-2011A [10, 11] and SLA, see also Refs. [28] and [31].

4. Summary

Photoproduction of K^0 on the deuteron showed up to be a useful tool for testing the dynamics of isobar models. Data for photoproduction of K^+ on the proton (or electroproduction with a very small Q^2) at very small kaon angles and for a wide energy region are needed to shed light on the angular and energy behavior of the cross section and the dynamics of isobar models in this kinematical region. Recent electroproduction data for very small Q^2 suggest that longitudinal couplings of the virtual photon to baryons in the effective Lagrangian are not too much important in the isobar models and that the models without the longitudinal couplings give also reasonable results for the electroproduction cross sections.

5. Acknowledgments

P.B. wants to express a tribute and special thanks towards his friends and colleagues Miloslav Sotona, who passed away on 6th April, 2012, and Osamu Hashimoto, who passed away on 3rd February, 2012. I am very grateful to them for the numerous stimulating and helpful discussions and encouragement in my work. We would like to dedicate this work to their memory.

P.B. thanks also the organizers for their kind invitation to the conference. This report was supported by the Grant Agency of the Czech Republic, grant P203/12/2126. The work was also supported in part by the Research Infrastructure Integrating Activity “Study of Strongly Interacting Matter” HadronPhysics2 under the 7th Framework Programme of EU and by the Core-to-Core program of Japan Society for Promotion of Science.

References

- [1] P. Bydžovský, M. Sotona, T. Motoba, K. Itonaga, K. Ogawa, and O. Hashimoto, Nucl. Phys. A 881 (2012) 187; T. Motoba, P. Bydžovský, M. Sotona, and K. Itonaga, Prog. Theor. Phys. Suppl. 185 (2010) 224.
- [2] P. Bydžovský and T. Mart, Phys. Rev. C 76 (2007) 065202.

- [3] T. Mart and C. Bennhold, Phys. Rev. C 61 (1999) 012201(R); T. Mart, Phys. Rev. C 62 (2000) 038201.
- [4] P. Bydžovský and M. Sotona, Nucl. Phys. A 754 (2005) 243c.
- [5] W.T. Chiang, F. Tabakin, T.-S.H. Lee, and B. Saghai, Phys. Lett. B 517 (2001) 101; G. Penner and U. Mosel, Phys. Rev. C 66 (2002) 055212; B. Julia-Diaz, B. Saghai, T.-S. Lee, and F. Tabakin, Phys. Rev. C 73 (2006) 055204; R. Shyam, O. Scholten, and H. Lenske, Phys. Rev. C 81 (2010) 015204.
- [6] J.C. David, C. Fayard, G.-H. Lamot, and B. Saghai, Phys. Rev. C 53 (1996) 2613.
- [7] T. Mart, C. Bennhold, H. Haberzettl, and L. Tiator, <http://www.kph.uni-mainz.de/MAID/kaon/kaonmaid.html>.
- [8] S. Janssen, J. Ryckebusch, D. Debruyne, and T. Van Cauteren, Phys. Rev. C 65 (2001) 015201.
- [9] T. Corthals, J. Ryckebusch, and T. Van Cauteren, Phys. Rev. C 73 (2006) 045207; T. Corthals, T. Van Cauteren, J. Ryckebusch, and D.G. Ireland, Phys. Rev. C 75 (2007) 045204; T. Corthals, T. Van Cauteren, P. Vancraeyveld, J. Ryckebusch, and D.G. Ireland, Phys. Lett. B 656 (2007) 186;
- [10] L. De Cruz, T. Vranckx, P. Vancraeyveld, and J. Ryckebusch, Phys. Rev. Lett. 108 (2012) 182002.
- [11] L. De Cruz, PhD Thesis, Ghent University, 2011.
- [12] M. Guidal, J.-M. Laget, and M. Vanderhaeghen, Nucl. Phys. A 627 (1997) 645.
- [13] B. Saghai, in *Proc. of Electrophotoproduction of Strangeness on Nucleons and Nuclei*, Sendai, Japan, 16-18 June, 2003, (Eds. K.Maeda, H.Tamura, S.N.Nakamura, O.Hashimoto). World Scientific, 2004, p. 53.
- [14] T. Mizutani, C. Fayard, G.-H. Lamot, and B. Saghai, Phys. Rev. C 58 (1998) 75.
- [15] R.M. Davidson and R. Workman, Phys. Rev. C 63 (2001) 025210.

- [16] L. De Cruz, D.G. Ireland, P. Vancraeyveld, and J. Ryckebusch, Phys. Lett. B694 (2010) 33.
- [17] K. Tsukada et al, Phys. Rev. C 78 (2008) 014001, *ibid.* 83 (2011) 039904(E).
- [18] P. Bydžovský, M. Sotona, O. Hashimoto, and T. Takahashi, arXiv:nucl-th/0412035.
- [19] A. Bleckmann et al, Z. Phys. 239 (1970) 1.
- [20] K.-H. Glander et al, Eur. Phys. J. A 19 (2004) 251.
- [21] R. Bradford et al, Phys. Rev. C 73 (2006) 035202.
- [22] M. Sumihama et al, Phys. Rev. C 73 (2006) 035214.
- [23] A.M. Boyarski et al, Phys. Rev. Lett. 22 (1969) 1131.
- [24] P. Markowitz and A. Acha, Int. J. Mod. Phys. E 19 (2010) 2383.
- [25] B. Dey and C.A. Meyer, arXiv:1106.0479[hep-ph].
- [26] C.N. Brown et al, Phys. Rev. Lett. 28 (1972) 1086.
- [27] M. Iodice et al, Phys. Rev. Lett. 99 (2007) 052501; F. Cusanno et al, Phys. Rev. Lett. 103 (2009) 202501.
- [28] P. Achenbach et al, Eur. Phys. J. A48 (2012) 14.
- [29] G. Niculescu et al, Phys. Rev. Lett. 81 (1998) 1805.
- [30] R.M. Moring et al, Phys. Rev. C 67 (2003) 055205.
- [31] P. Achenbach et al, Nucl. Phys. A 881 (2012) 187.